# Creep-Fatigue Behavior of Additively Manufactured Inconel 718: Mechanisms and Challenges

Sujit B. Chaudhari
*Research Scholar, Dept. of Mechanical Engineering*
*Amrutvahini College of Engineering,*
Sangamner 422608, Maharashtra, India
Email: sujit.chaudhari@live.in

Vishnu D. Wakchaure
*Department of Mechanical Engineering*
*Amrutvahini College of Engineering,*
Sangamner 422608, Maharashtra, India

Ravindra E. Gite
*Department of Mechanical Engineering*
*Amrutvahini College of Engineering,*
Sangamner 422608, Maharashtra, India

***Abstract*: This review critically examines the creep-fatigue behavior of additively manufactured (AM) Inconel 718, emphasizing distinctions from conventionally processed forms due to unique microstructures and process-induced defects. Beginning with an overview of creep-fatigue mechanisms and test methods, the paper explores how AM processes such as SLM, EBM and DED produce columnar grains, Laves and δ phases, anisotropy and porosity—features that significantly affect cyclic softening, stress relaxation and crack growth.**

**The influence of post-processing treatments, including solution annealing, aging and HIP, is analyzed in terms of phase evolution, defect mitigation and performance under high-temperature loading. Fracture behavior is reviewed across different loading modes, build orientations and defect types, highlighting mixed-mode crack propagation and the role of grain morphology and residual stress.**

**A detailed evaluation of life prediction models, including strain-based, energy-based and hybrid approaches, underscores the need for AM-specific frameworks capable of capturing anisotropic and time-dependent damage. Unlike previous reviews that have primarily focused either on conventional Inconel 718 or on general fatigue and creep studies, this review consolidates creep-fatigue findings specific to AM Inconel 718, integrates insights on microstructural effects, post-processing strategies and life prediction models, and identifies critical gaps for AM-tailored design standards. Key research gaps are identified including the lack of standardized testing, limited understanding of defect criticality and inadequate post-processing guidelines.**

**The review concludes with proposed directions for advancing AM Inconel 718 reliability, including the development of representative datasets, improved testing standards, microstructural mapping and scalable life prediction tools.**

***Keywords*: *Additive Manufacturing, Inconel 718, Creep-Fatigue Interaction, Microstructure, Residual Stress, Life Prediction Models, Post-Processing***

## I. INTRODUCTION

The aerospace and power generation industries' unrelenting quest for improved performance and efficiency has elevated additively produced (AM) Inconel 718 components to the forefront of material innovation. Because of its remarkable mechanical qualities, resistance to oxidation and high strength at high temperatures, Inconel 718, a nickel-based superalloy, has become an essential component for high-temperature applications [1]. It is extensively utilized in demanding industries including gas turbines, power generation and aerospace where parts must withstand high mechanical and thermal strains. The alloy is an excellent alternative for parts like turbine blades, engine parts and nuclear reactor components where performance and dependability are crucial under demanding operating conditions because of its high yield strength, outstanding corrosion resistance and good creep resistance [2], [3]. Complex Inconel 718 components are now possible to manufacture with shorter lead times and less material waste thanks to the development of additive manufacturing (AM) technologies. AM techniques, like directed energy deposition (DED), electron beam melting (EBM) and selective laser melting (SLM), provide design flexibility and the capacity to create complex geometries that are difficult to accomplish with traditional production processes [4]. However, these benefits come with unique challenges. Because AM methods employ layer-by-layer fabrication and experience rapid cooling rates, they result in distinct microstructural features, including columnar grains, high residual stresses and potential defects like porosity and lack of fusion. These microstructural characteristics, such as anisotropic grain structures promoting preferential crack paths, or residual stresses that can either accelerate or retard damage accumulation, introduce complexities to creep-fatigue behavior not typically encountered in their conventionally manufactured counterparts [5]. In high-temperature applications, components are often exposed to simultaneous cyclic mechanical loading and prolonged thermal exposure, leading to creep-fatigue interaction (CFI). This phenomenon is particularly critical for AM Inconel 718, where the interplay between creep and fatigue can severely impact long-term component reliability [6]. Microstructure, temperature, loading conditions and environmental factors all have a significant impact on the complex failure mechanisms that occur from the combined impacts of time-dependent creep deformation and cyclic fatigue damage. Accurately estimating the service life of AM components requires an understanding of these interactions, particularly in safety-critical applications where unplanned breakdowns could have disastrous results, such as jet engines and power turbine [7]. Given the increasing reliance on AM technologies for producing Inconel 718 components, there is a growing need to systematically review and synthesize the current understanding of creep-fatigue behavior in this material [4]. While considerable research has been conducted on conventionally manufactured Inconel 718, relatively few studies have focused on the unique challenges presented by

the AM variants. This review aims to give researchers and engineers a better grasp of the state-of-the-art by offering a comprehensive overview and critical analysis. It also hopes to encourage additional developments in order to guarantee the long-term dependability of AM Inconel 718 components under demanding service conditions.

By critically analyzing the body of research on the creep-fatigue interaction of Inconel 718 that has been additively manufactured, this review seeks to close this gap. This paper is organized as follows: A thorough overview of creep-fatigue interaction processes and testing methodologies, with an emphasis on nickel-based superalloys, is given in the introduction section. The special microstructural characteristics of AM Inconel 718 and how they affect mechanical performance are covered in Section 2. The impacts of flaws, anisotropy and residual stresses are reviewed in Section 3 along with the state of knowledge about creep-fatigue behavior in AM Inconel 718. Section 4 explores crack growth behavior and fracture mechanisms under creep-fatigue conditions, while Section 5 covers life prediction models and computational approaches. The article concludes with an assessment of significant knowledge gaps, possible research directions and practical challenges in improving AM Inconel 718's creep-fatigue performance.

### *A. Fundamentals of Creep-Fatigue Interaction*

Superalloys based on nickel, especially Inconel 718, are widely employed in high-temperature applications because of their exceptional mechanical qualities, which include high strength, resistance to oxidation and thermal stability [2]. Understanding the material's performance in service, especially with regard to creep and fatigue mechanisms, depends on how it behaves when exposed to high temperatures for an extended period of time. The life expectancy of components constructed from these alloys under service circumstances is significantly influenced by the interaction between these two failure modes, known as the creep-fatigue interaction [8]When a material is subjected to constant stress at elevated temperatures—typically exceeding 40% of its melting temperature—it experiences creep, a deformation that occurs over time. This process progresses through three distinct stages: primary (characterized by a decreasing creep rate), secondary (marked by a steady creep rate) and tertiary (where the creep rate accelerates, leading to failure). In the case of Inconel 718, the primary mechanisms responsible for creep include grain boundary sliding, the coarsening of precipitates and the movement of dislocations through glide and climb [9]. As temperature increases, the diffusion of atoms accelerates, contributing to the movement of dislocations and the onset of creep deformation. The coarsening of precipitates, including the γ' phase in Inconel 718, significantly contributes to the material's degradation at high temperatures, ultimately resulting in creep failure [10]. On the other hand, fatigue refers to the material's behavior under repeated cyclic loading. Even when the applied stress is below the ultimate tensile strength, such loading can lead to the initiation and growth of microscopic cracks over time. In nickel-based superalloys, fatigue typically originates at stress concentrators like grain boundaries or the interfaces between precipitates and the matrix, with cracks progressively propagating under cyclic stress [11]. The fatigue resistance of a material is influenced by several factors, including grain structure, operating temperature and the presence of internal flaws or inclusions. Inconel 718 demonstrates strong resistance to both creep and fatigue due to its precipitation hardening and solid solution strengthening. However, when creep and fatigue occur concurrently—such as in high-temperature applications like turbine blades—the interaction between the two mechanisms becomes complex and accelerates material degradation. Creep-fatigue interaction arises under combined high-temperature and cyclic loading conditions, where cyclic stresses enhance creep damage accumulation and creep deformation, in turn, facilitates fatigue crack growth. This interplay often results in more severe damage than would occur from either mechanism independently [7]. Components like boiler tubes, pressure vessels and turbine blades, where varying stresses and thermal loads are a common part of operation, are especially vulnerable to this kind of combined degradation.

TABLE I. SCHEMATIC REPRESENTATIONS OF TYPICAL CREEP-FATIGUE TESTING WAVEFORMS [12]

| Scheme No. | Name | Schematic of Waveform |
|---|---|---|
| 1.Variable strain rate low-cycle fatigue (VSRLCF) | Slow-fast | 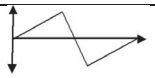 |
| | Fast-slow | 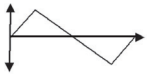 |
| | Slow relaxation from 0.6% to 0.4% at 1000s | 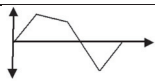 |
| 2. Nonpeak & nonpeak-peak mixed | Nonpeak tensile | 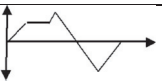 |
| | Nonpeak compressive | 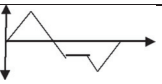 |
| | Peak tensile + nonpeak tensile | 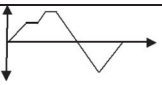 |
| | Peak tensile + nonpeak compressive | 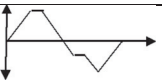 |
| | Nonpeak tensile + peak compressive | 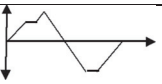 |
| 3. Standard peak hold | Peak compressive | 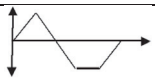 |
| | Peak tensile | 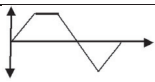 |
| | Both hold | 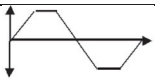 |

Testing methods for creep-fatigue interaction are typically designed to simulate these operational realities, incorporating both strain-controlled cyclic loading and time-dependent dwell periods. Standard test protocols often include strain-controlled low-cycle fatigue (LCF) experiments, with modifications to introduce dwell periods at peak or nonpeak strain values. These dwell times allow for stress relaxation and creep deformation, enabling assessment of time-

dependent effects. In addition to conventional symmetric waveforms, more complex loading patterns—such as slow-fast or fast-slow ramp rates, strain gradients and mixed peak-nonpeak dwell distributions—are employed to mimic real-world transients. Key input parameters in these tests include strain amplitude, strain rate, waveform shape and dwell duration. Table I illustrates broader classification of waveform types and their variations.

Output measurements typically consist of stress response (including amplitude and mean stress evolution), cyclic softening behavior, hysteresis loop characteristics (such as inelastic strain range and energy dissipation) and total fatigue life.

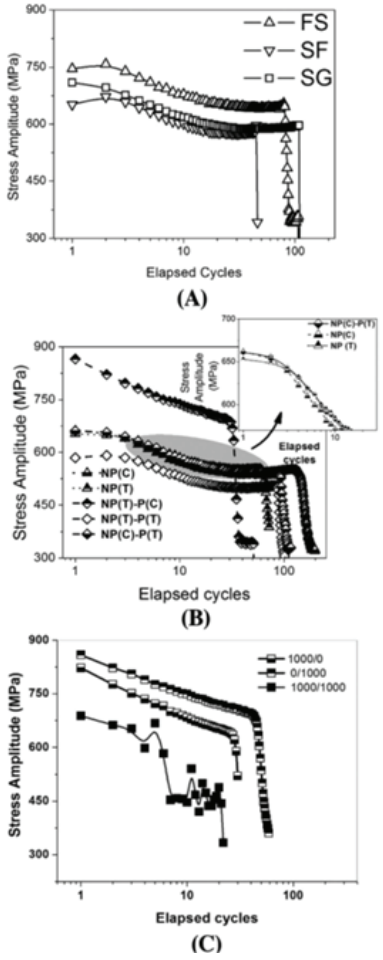


Fig. 1: Variation in stress amplitude of Inconel 718 during creep-fatigue interaction tests conducted under different waveform profiles. The plots illustrate cyclic softening behavior in most cases, with differences in softening rate and stabilization depending on waveform type (e.g., slow-fast, fast-slow, peak dwell, nonpeak dwell) [12].

**The stress response** is material's reaction to applied strain under varied waveform conditions and multiple loading cycles. It takes into account the material's overall stress-strain behavior during the test as well as the evolution of peak stress levels.

**Cyclic softening behaviour** is a prominent feature in creep-fatigue interaction, where the material exhibits a progressive reduction in stress amplitude under constant strain-controlled cycling. This behavior reflects microstructural degradation mechanisms such as dislocation rearrangement, sub-grain formation and precipitate shearing, especially at elevated temperature. The behavior is quantified using the degree and rate of softening. The degree of softening is calculated as

$$\text{Degree of Softening} = \frac{\Delta\sigma_1 - \Delta\sigma_{sat}}{\Delta\sigma_{sat}}$$

where $\Delta\sigma_1$ represents stress range during the first cycle and $\Delta\sigma_{sat}$ denotes stress range at saturated or stabilized cycle.

**The rate of softening** is determined by calculating the derivative of the peak tensile stress with respect to the number of cycles within the stabilized regime of the test. In cases without clear stabilization, the mid-life point ($N_f/2$) is used as a reference. This parameter reflects how rapidly the material undergoes stress degradation during cyclic loading and correlates inversely with fatigue life. The cyclic softening behaviour and rate of softening are illustrated in Fig. 2.

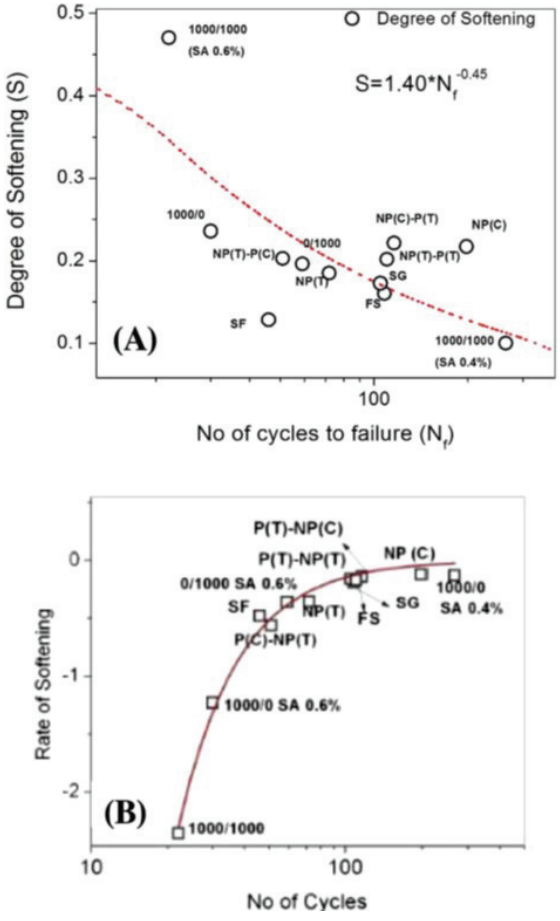


Fig. 2: Trends in softening behavior of Inconel 718 under various waveform-induced creep-fatigue loading conditions — (A) Degree of softening and (B) Softening rate plotted against fatigue life [12].

In creep-fatigue testing, stress vs. inelastic strain hysteresis loops are a critical output parameter used to characterize the material's cyclic deformation behavior. These loops reflect the energy dissipation, accumulation of irreversible strain and the nature of time-dependent deformation mechanisms. Hysteresis loops plotted between stress and inelastic strain provide valuable information about the material's deformation response under cyclic and time-dependent loading. The loop width represents the inelastic strain amplitude, which includes both plastic and creep contributions. The area of the loop corresponds to the inelastic energy density dissipated in a cycle. Fig. 3. Illustrates stress vs. inelastic strain hysteresis loops for

Inconel 718 under different waveform-based creep-fatigue loading schemes.

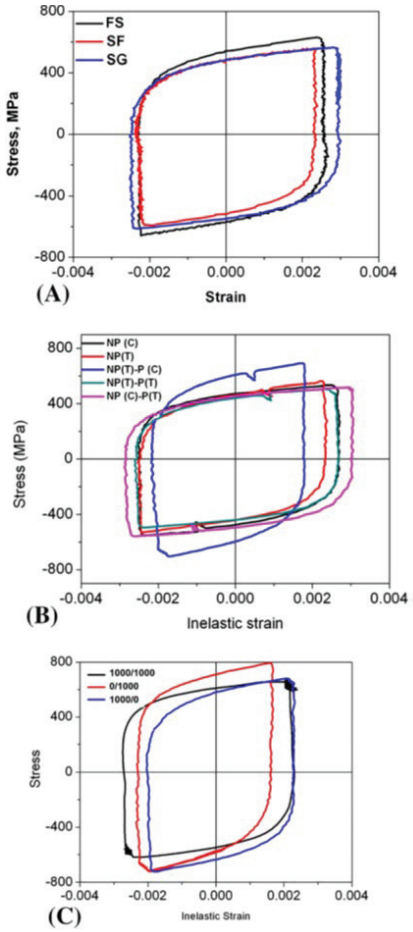


Fig. 3. Representative stress vs. inelastic strain hysteresis loops for Inconel 718 under different waveform-based creep-fatigue loading conditions [12].

Numerous models have been proposed to assess and predict damage resulting from creep-fatigue interactions. These include strain-based models, energy-based approaches that relate inelastic strain energy to fatigue life and fracture mechanics-based parameters that incorporate both plastic and creep deformation contributions. Additionally, methods that decompose total energy into plastic and creep components provide further insight into dominant damage mechanisms. Collectively, these testing methodologies and modeling strategies form the basis for evaluating material behavior under creep-fatigue interaction and guiding the design of components intended for high-temperature service environments.

## II. ADDITIVE MANUFACTURING OF INCONEL 718

Inconel 718, a commonly utilized nickel-based superalloy, is being adopted more frequently for production through Additive Manufacturing (AM) methods due to its good weldability and the design freedom offered by AM [13], [14]. This section explores common AM processes for Inconel 718, typical microstructural features arising from these processes and the post-processing methods employed to optimize material properties.

### *A. Overview of Additive Manufacturing Processes for Inconel 718*

Several AM technologies are utilized for Inconel 718, broadly falling under categories like Powder Bed Fusion (PBF) and Directed Energy Deposition (DED) [15].

Selective Laser Melting (SLM): A PBF process where a laser selectively fuses powder particles layer by layer [14], [15]. Machines like the EOSINT M280 and SLM 280 HL are used. Selective Laser Melting (SLM) enables the fabrication of near fully dense components with intricate geometries in a single manufacturing step. The process often involves high cooling rates and temperature gradients [16], [17].

Laser Beam Directed Energy Deposition (LB-DED): In this technique, a laser generates a melt pool while powder is concurrently deposited and melted, allowing material to be built up layer by layer and track by track. The OPTOMEC LENS™ 750 system serves as an example of LB-DED technology [13].

Electron Beam Melting (EBM): Another PBF process, utilizes an electron beam as its primary energy source for melting the metal powder. EBM can produce a columnar-grained microstructure with a pronounced texture, which can be beneficial for high-temperature applications. Systems like Arcam A2X are used for EBM of Inconel 718 [1].

These AM processes enable the creation of Inconel 718 components exhibiting unique microstructures that deviate considerably from those observed in conventionally wrought or cast materials.

### *B. Microstructural Features Specific to AM Inconel 718*

The rapid solidification inherent in AM processes induces distinct microstructural characteristics in Inconel 718:

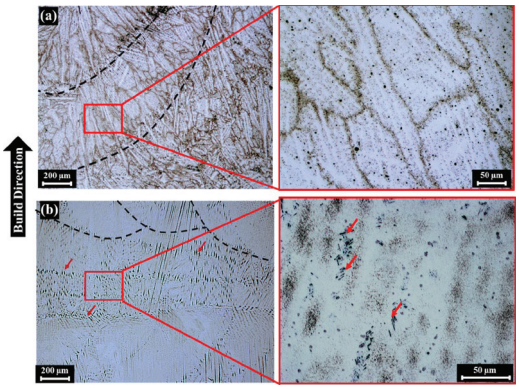


Fig. 4: Microstructures in (a) as-built and (b) AMS 5596C heat-treated conditions, with fusion zones (black dashed lines) and needle-like δ phases (red arrows) [13].

Columnar and Dendritic Grains: Additively manufactured Inconel 718 often displays columnar grain structures oriented along the build direction (BD), a result of the directional heat dissipation inherent to the process [1], [13]. Dendritic structures are commonly observed within these grains, particularly in as-built LB-DED and SLM parts [14]. It is noted that heat treatments may not completely eliminate these dendritic morphologies [13]. Fig. 4 provides a visual representation of the as-built dendritic structure in LB-DED IN718.

Laves and Delta (δ) Phases: During rapid solidification, micro-segregation of elements like Niobium (Nb) commonly occurs, resulting in the formation of Nb-rich Laves phases

($(Ni,Fe,Cr)_2(Nb,Mo,Ti)$) within interdendritic areas or along grain boundaries [13], [14], [18]. These Laves phases are often characterized by an irregular morphology and brittleness. [14]. Intact Laves phases can impede crack propagation, but they can act as preferential crack paths if fragmented [18]. Fig 5 (a) provides a good illustration of Laves phases. The δ phase ($Ni_3Nb$), typically exhibiting a needle-like morphology, can also precipitate along grain and cell boundaries, especially following specific heat treatments [13], [17]. Fig. 6 (d) shows extensive grain boundary precipitation, likely including the δ phase, in Hot Isostatically Pressed (HIP'd) Laser Powder Bed Fusion (LPBF) IN718.

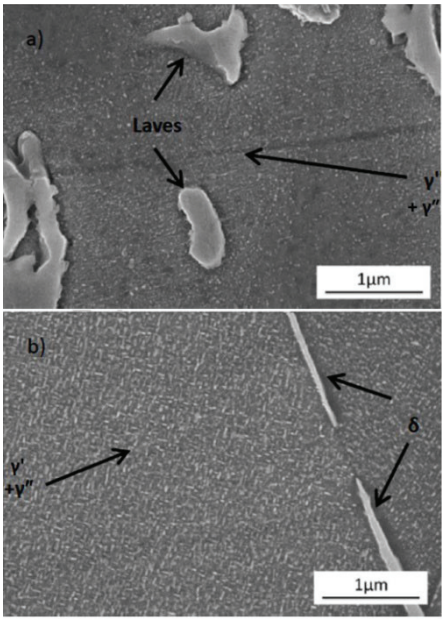


Fig. 5 Microstructure: (a) LAMed; (b) Wrought Inconel 718 [18].

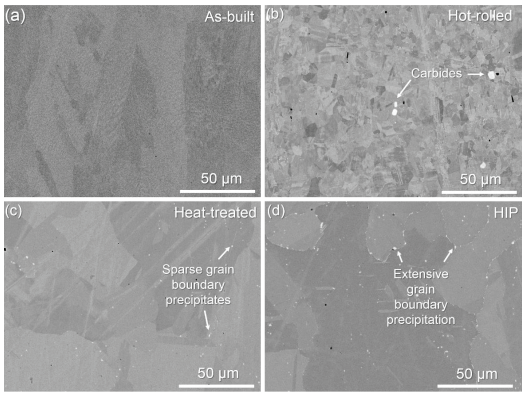


Fig. 6: SEM micrographs of (a) as-built, (b) hot-rolled, (c) heat-treated (HT) and (d) hot isostatically pressed (HIP) specimens perpendicular to the build direction, highlighting grain boundary precipitates [19].

Strengthening Phase Precipitation (γ′, γ″): The fast cooling associated with as-built Powder Bed Fusion–Laser Beam Melting (PBF-LB/M) conditions can suppress the precipitation of the key strengthening phases γ″ ($Ni_3Nb$) and γ′ ($Ni_3(Al,Ti)$) [17]. Consequently, post-process heat treatments are critical for the precipitation of these phases. In Laser Additive Manufactured (LAMed) material, γ″ phases can preferentially precipitate in the vicinity of Laves phases [18]. Fine γ′ and γ″ precipitates are seen in the cellular substructures of Electron Beam Melted (EBM) Inconel 718 after hot isostatic pressing (HIP) and thereafter heat treatment (HT). [1]. Fig. 7 (b) shows γ″ precipitates of region marked in 7 (a). Fig. 8 shows γ′ and γ″ in Solution Annealed (SA) and Homogenization and Aging (HA) samples.

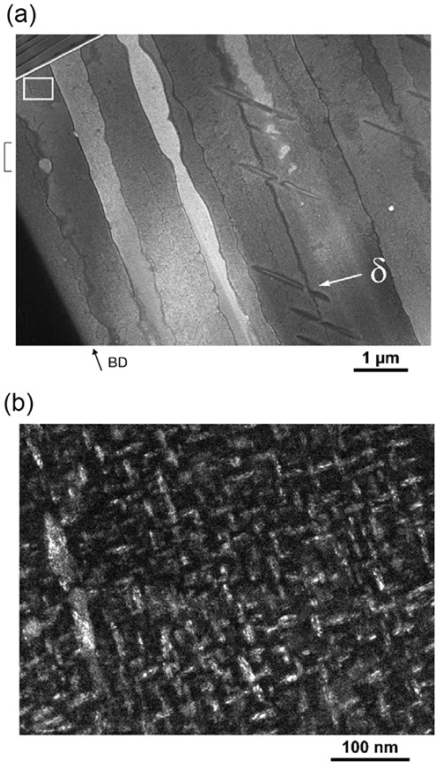


Fig. 7 SEM image (a) STEM-BF image (1 μm) with marked region; (b) γ″ precipitates from the extracted FIB lamella [17].

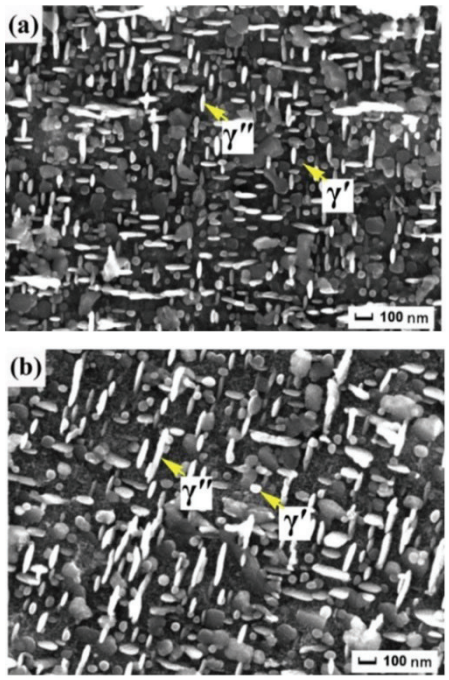


Fig. 8: SEM images showing circular γ′ precipitates and plate-like γ″ phases. in (a) Solution Annealed and (b) Homogenization plus double aging specimen [14].

Anisotropy and Heterogeneity: AM-fabricated parts often exhibit anisotropic mechanical behavior due to the development of textured and oriented microstructures relative to the build direction [15]. LBPF IN718 can display a heterogeneous yet periodic grain structure, characterized by regions of predominantly elongated grains (PEGM) and

columns of stacked grains with ripple patterns (SGWRP) [17].

Porosity and Defects: While AM processes aim to achieve full density, a certain level of porosity, which can manifest as gas porosity or lack-of-fusion defects, may be present. These defects can negatively impact mechanical properties, particularly fatigue performance [17].

The mechanical behavior of additively manufactured Inconel 718 is governed by the collective effects of various microstructural characteristics, such as grain size, morphology, phase distribution and the presence of defects. For instance, under creep loading, laser powder bed fusion (LPBF) samples frequently exhibit intergranular fracture as the primary failure mode, largely driven by the presence of precipitates along grain boundaries. [19].

### *C. Post-Processing Methods*

Post-processing approaches, particularly HT and HIP, are essential for homogenizing the microstructure, relieving residual stresses, precipitating strengthening phases and mitigating defects such as porosity. A range of heat treatment approaches are utilized to modify and optimize the microstructure of additively manufactured Inconel 718:

*1) Direct Aging (DA):* This approach is utilized in some LAM processes to retain specific microstructural features, such as Laves phases, which might be desirable when subsequent high-temperature solutioning is not feasible (e.g., for repaired components) [18].

*2) Solution Annealing and Aging (SA/STA):* This common strategy involves a solution treatment to dissolve segregated phases and promote matrix homogenization, followed by aging steps to precipitate γ′ and γ″ phases. Examples include:

a) *LB-DED IN718* annealed at 940°C, followed by a double aging treatment at 718°C and 621°C. This evidently reduced the presence of dendritic structures, though they were not entirely removed and promoted the development of elongated, needle-like δ phase precipitates [13].

b) *SLM IN718* solution treatment at 980°C, followed by a double aging process at 760°C and 650°C. This heat treatment led to the formation of Laves and δ phases along grain boundaries, along with the precipitation of fine γ′/γ″ strengthening phases [14].

*3) Homogenization, Solution Annealing and Aging (HA):* This often involves an initial high-temperature homogenization step. It incorporates homogenization at 1065°C followed by twofold aging at 760°C and 650°C. This dissolved δ phases (due to homogenization above the δ solvus temperature) but retains Laves phases, leading to larger γ′/γ″ precipitates and improved creep life compared to the SA treatment [14].

*4) Hot Isostatic Pressing (HIP):* It is employed to reduce or eliminate internal porosity and can also influence the resulting microstructure. It involves HIP at 1200°C under 103 MPa for 240 minutes. While HIP effectively closed pores, sometimes it may cause extensive intergranular precipitation, resulting in a decline in creep performance in comparison to both the conventional heat-treated circumstances and the as-built conditions. [19]. This can be visualized from Fig. 6 (d) showing extensive grain boundary precipitation in HIPed samples as compared to sparse boundary precipitation in Heat treated samples as shown in Fig. 6 (c).

The microstructure of Inconel 718 is shaped by the Additive Manufacturing (AM) technique and the associated post-processing treatments, which ultimately determine the material's mechanical performance. This allows the material to be customized to meet the needs of particular applications. However, replicating a microstructure that performs on par with or better than its wrought equivalents across all important characteristics is still a difficult and developing goal.

Optimization of post-processing treatments is essential to balance microstructural refinement with creep-fatigue resistance. In heat-treated AM Inconel 718, controlling δ-phase precipitation and avoiding excessive grain coarsening are critical, since both can degrade crack growth resistance. Similarly, while HIP effectively reduces porosity, scaling it to industrial production involves trade-offs in cost, energy demand, and reproducibility across large or complex geometries. These factors underline the need for optimized post-processing strategies that support reliable creep-fatigue performance in service conditions.

## III. CREEP-FATIGUE CHALLENGES IN ADDITIVELY MANUFACTURED INCONEL 718: THE ROLE OF MICROSTRUCTURE AND RESIDUAL STRESSES

SLM, DED, EBM and other additive manufacturing (AM) techniques allow for the creation of complex Inconel 718 components with microstructures that differ greatly from those made by traditional casting or forging. [4]. The rapid, localized melting and solidification inherent to these AM processes produce directional, columnar grains oriented in the direction of the build, fine dendritic structures and characteristic cellular solidification patterns. This microstructural anisotropy, combined with high cooling rates, leads to the development of different phases, including Laves phases and carbide precipitates, which can embrittle the alloy and impact its high-temperature performance [5], [20]. Moreover, AM components typically exhibit high residual stresses due to rapid thermal cycling and non-uniform cooling, which can affect creep and fatigue behavior [21]. Tensile residual stresses near the surface can accelerate crack initiation and growth under cyclic loading, while internal compressive stresses may provide localized strengthening but at the cost of increased brittleness. These stresses can also interact with microstructural defects like porosity, lack of fusion and unmelted particles, all of which act as early crack initiation sites, significantly reducing both creep resistance and fatigue life [22], [23]. The interplay between these features and creep-fatigue interaction is complex. For example, columnar grains can promote anisotropic mechanical behavior, leading to uneven creep deformation and directional crack growth. At the same time, fine cellular structures, while beneficial for tensile strength, can accelerate creep cavity formation at grain boundaries under sustained high temperatures [24]. The occurrence of brittle Laves phases, formed due to high cooling rates, can also act as crack initiation sites, further compromising fatigue resistance.

TABLE II. KEY FINDINGS FROM EXPERIMENTAL CREEP-FATIGUE STUDIES IN AM INCONEL 718 AND CONVENTIONAL NICKEL-BASED SUPERALLOYS

| Material | Processing / AM Technique | Test Conditions | Focus Area | Key Findings | Reference |
|---|---|---|---|---|---|
| Inconel 718 | Conventional + dataset | LCF + CFI, multiple T & strain ratios | Data-driven & physics-informed model | New symbolic regression model predicts life more accurately than existing ones | Gu et al., [29] |
| HAYNES 282 | Wrought | 760°C, trapezoidal waveform, tensile/compressive/both dwell | Dwell position & time effect | Damage order: both-dwell > compressive > tensile; fracture mode changes with dwell | Mukherjee et al., [30] |
| Inconel 718 | EBM (Additive Manufacturing) | 300–650°C, TMF & LCF, dwell/slow-fast cycles | Creep-fatigue under AM processing | Columnar <001> texture improves resistance; dwell cycles → intergranular cracking; better life than wrought | Guth et al., [1] |
| GH4169 (≈ IN718) | Conventional | 650°C, tension-hold tests | Cycle-by-cycle prediction model | Strain energy density exhaustion model gives higher accuracy than traditional | Wang et al., [31] |
| GH4169 | Conventional | 650°C, tensile hold up to 120s | LCF & CFI life | Life decreases with hold (≤120s); cyclic softening observed; mixed brittle–ductile fracture | Chen et al., [32] |
| XH73M | Conventional | 23–750°C, triangular/trapezoidal cycles | Crack growth under CFI | CFI accelerates crack growth; intergranular fracture dominates at ≥550°C | Shanyavskiy et al., [33] |
| GH4169 + FGH96 | Conventional / PM | 650°C, tensile & compressive dwell | Walker strain equation-based model | New model captures dwell & load ratio; good prediction within 2× scatter band | Chen et al., [34] |
| DZ125 | Cast superalloy (blade) | 980°C, turbine blade service conditions | Life prediction (damage mechanics) | MKRC model predicts life with ~3% error; fracture shows micro-cracks & pores | Sun et al., [35] |
| Various superalloys | Mixed (Ni, Co, Fe-based) | Different T, strain, dwell | Review of CFI studies | Tensile dwell most damaging; higher T & strain amplitude reduce life | Jadon et al., [7] |

A variety of post-processing techniques are used to enhance Inconel 718's mechanical performance and creep-fatigue resistance in order to overcome the microstructural issues brought about by additive manufacturing. Hot Isostatic Pressing (HIP) for example, is widely employed to minimize internal porosity and reduce micro-cracks through the application of high pressure and temperature, which enhances ductility and extends fatigue life. [25]. This process also promotes microstructural homogenization, reducing the number of high-stress concentration sites that can accelerate creep cavity formation. Heat treatments, including solution annealing and aging, are crucial for dissolving detrimental Laves phases and promoting the growth of the more desirable γ' and γ" strengthening phases[26], [27]. These phases provide significant creep resistance by impeding dislocation motion, thus enhancing both high-temperature strength and fatigue resistance. Surface finishing methods, like shot peening or laser shock peening, are also employed to introduce surface-level compressive residual stresses, thereby delaying crack initiation and slowing crack growth under fluctuating loading conditions [28]. These methods are especially useful for lowering the possibility of premature failure under combined creep-fatigue loading by minimizing the tensile residual stresses that frequently occur during production. Collectively, these post-processing treatments are vital for refining the microstructure, minimizing sensitivity to defects and enhancing the creep-fatigue life of additively manufactured Inconel 718—establishing it as a dependable material for demanding aerospace and power generation applications. Understanding these AM-specific influences is essential for accurate life prediction and safe component design.

While the present work specifically focuses on additively manufactured Inconel 718, the body of literature on creep-fatigue interaction in AM Inconel 718 is still limited. Therefore, insights from studies on other nickel-based superalloys such as HAYNES 282, GH4169, FGH96, XH73M, and DZ125 are also included. These alloys share similar strengthening mechanisms (γ′/γ″ precipitation hardening) and exhibit comparable deformation and damage behaviors at elevated temperatures. Lessons drawn from these studies not only broaden the understanding of creep-fatigue interaction mechanisms but also provide useful context for interpreting the results on Inconel 718. Table II highlights material type, processing route, test conditions, focus areas and key findings, thereby offering a consolidated overview that complements the descriptive discussion in the text.

## IV. CRACK GROWTH AND FRACTURE BEHAVIOUR

When evaluating the durability of additively produced (AM) Inconel 718 in conditions with high temperatures and cyclic stress, the crack initiation, propagation and fracture characteristics are crucial. This section investigates the fundamental processes that govern the formation of cracks in creep, fatigue and combined creep-fatigue scenarios. It also looks at how defects affect fracture behavior and how loading and temperature affect it.

### *A. Mechanisms of Crack Initiation and Propagation*

Microstructural characteristics like grain boundaries, precipitates and defects like pores or unmelted particles are usually where cracks start. Intergranular fracture results from the nucleation and coalescence of voids at grain boundaries, which is how cracks often begin under creep circumstances. At elevated temperatures, this process is accelerated due to enhanced atomic diffusion and grain boundary sliding [36]. For instance, early stages of creep void development along grain boundaries, followed by void coalescence and crack formation, have been observed in high-temperature creep tests [37]. Fig. 9 illustrates a typical crack path under combined creep-fatigue loading, highlighting the alternating nature of crack propagation in this complex environment.

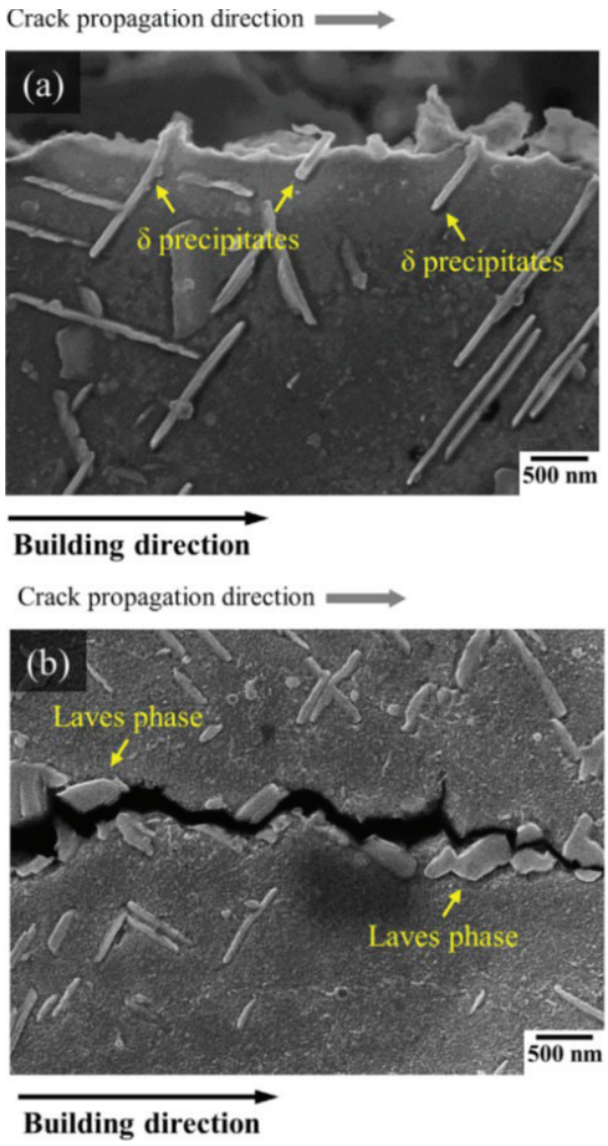


Fig. 9: Typical crack path under combined creep-fatigue loading, highlighting both intergranular and transgranular crack features [36].

Under purely fatigue loading conditions, crack initiation is primarily driven by cyclic slip at stress concentrators like surface irregularities and internal pores, leading to transgranular crack propagation [38]. Additionally, the presence of inclusions, particularly in EB-PBF processed Inconel 718, can significantly reduce fatigue life by promoting early crack initiation [39]. In low cycle fatigue (LCF) testing, crack initiation has been noted at these inclusions, followed by rapid propagation through the matrix material. [40]. Additionally, microstructural anisotropy, particularly along the building direction, has a strong influence on crack growth, with vertically built samples showing faster crack propagation due to aligned columnar

grains [41]. Fig. 10 illustrates this orientation-dependent crack growth behavior. Vertically built samples Fig. 10 (a) exhibit predominantly transgranular cracking with relatively straight crack paths, minimal branching and limited grain boundary interaction, leading to faster crack growth. In 45° built samples Fig. 10 (b), cracks show more deviation, mixing transgranular and intergranular mechanisms, with significant branching at grain boundaries. Horizontally built samples Fig. 10 (c), exhibit highly tortuous paths, with predominant intergranular cracking and significant crack twisting, resulting in slower crack propagation rates.

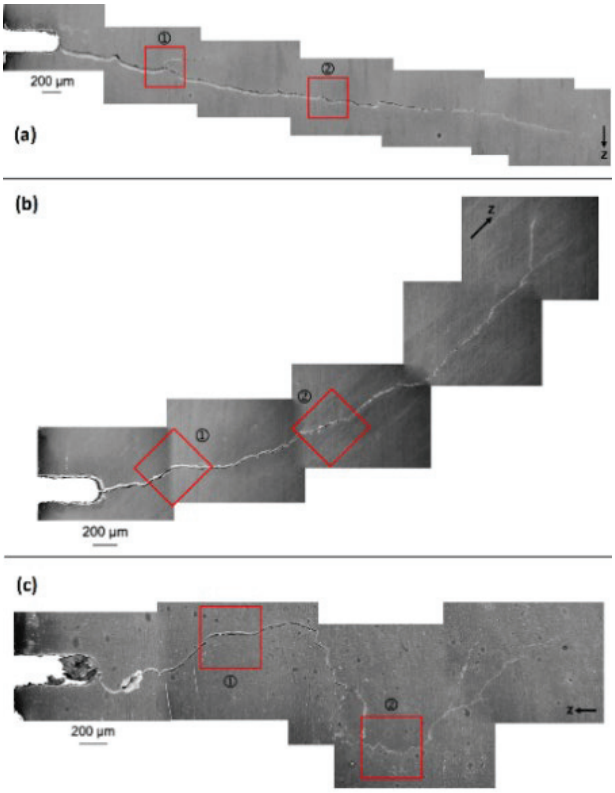


Fig. 10: SEM images of crack growth in L-PBF Inconel 718 specimens with different build orientations: (a) FV, XY-plane orthogonal to loading direction, (b) F45, XY-plane oriented at 45° to loading direction, and (c) FH, XY-plane parallel to loading direction. Distinct crack path morphologies are visible depending on orientation. [41].

In combined creep-fatigue conditions, crack propagation mechanisms are influenced by both time-dependent creep deformation and cyclic loading, resulting in a mixed-mode fracture. In this regime, cracks tend to grow along grain boundaries while also exhibiting features of transgranular fracture due to alternating loading [38]. High-temperature conditions further promote intergranular cracking due to grain boundary oxidation and embrittlement [37].

### *B. Effect of Defects on Crack Growth*

Defects such as porosity, un-melted particles, inclusions and microstructural heterogeneity significantly impact crack growth in AM Inconel 718. These defects act as stress concentrators, reducing the effective load-bearing area and promoting early crack initiation. For instance, studies have shown that un-melted powder particles, lack of fusion (LOF) pores and surface imperfections resulting from the additive manufacturing process contribute to lower fatigue life and reduced fracture toughness. [39]. High porosity and clustered defects can significantly reduce the fatigue crack growth threshold and increase crack propagation rates [42]. Additionally, the δ phase can serve as a barrier to crack tip plasticity, significantly affecting the material's resistance to crack propagation, especially at high-temperatures conditions [43].

### *C. Role of Temperature and Loading Conditions*

Temperature has a substantial impact on the crack growth characteristics of additively manufactured Inconel 718. At higher temperatures, crack growth rates generally increase as a result of decreased matrix strength, higher creep deformation and more rapid grain boundary oxidation. For example, at 650°C, the crack growth rates in AM Inconel 718 were found to be considerably more compared to room temperature, especially in the high-stress intensity factor regime [36]. High-frequency cyclic loading tends to favour transgranular crack propagation, while lower frequencies promote intergranular cracking due to enhanced oxygen diffusion along grain boundaries [37]. The fine-grained structures are more susceptible to grain boundary oxidation and embrittlement, while coarser grains show better fatigue resistance due to reduced grain boundary area [44].

### *D. Other Significant Aspects*

Additional factors influencing crack growth include the build orientation, grain size and post-processing treatments. Vertical build orientations often exhibit lower fatigue resistance due to the layer-by-layer structure, which introduces anisotropy and residual stresses [39]. Additionally, post-processing techniques such as HIP, HT have been shown to improve fracture toughness by reducing internal defects and homogenizing the microstructure [42]. The role of grain size is particularly critical, as larger grains promote transgranular crack growth, while finer grains enhance intergranular crack resistance [45]. The microstructure contains various critical phases, including γ', γ", δ and Laves phases, which significantly influence crack growth behavior. The γ' ($Ni_3(Al,Ti)$) and γ" ($Ni_3Nb$) phases are the main strengthening precipitates that obstruct dislocation movement, thereby enhancing resistance to both creep and fatigue. However, excessive precipitation can reduce ductility and promote crack initiation. The δ phase (Ni3Nb), typically forming along grain boundaries, can act as a crack arrestor by impeding crack tip plasticity, but excessive δ phase can embrittle the material, reducing its fracture toughness. Laves phases, which are brittle intermetallic compounds that form during solidification, can significantly influence crack growth by acting as stress concentrators, reducing fracture toughness and promoting early crack initiation, especially under high-temperature creep conditions. These phases act as localized stress concentrators, reducing fracture toughness and promoting early crack initiation, especially under high-temperature creep conditions [43]. Fig. 11 illustrates the role of Laves phases in triggering creep crack initiation by concentrating stress at the crack tip in AM Inconel 718, a critical factor in determining crack propagation resistance at elevated temperatures.

All things considered, fully understanding these mechanisms is essential to maximizing AM Inconel 718's performance in demanding applications. In order to lower defect concentrations, optimize microstructure and enhance this alloy's overall mechanical performance in high-stress, high-temperature settings, future research should concentrate on improving AM methods.

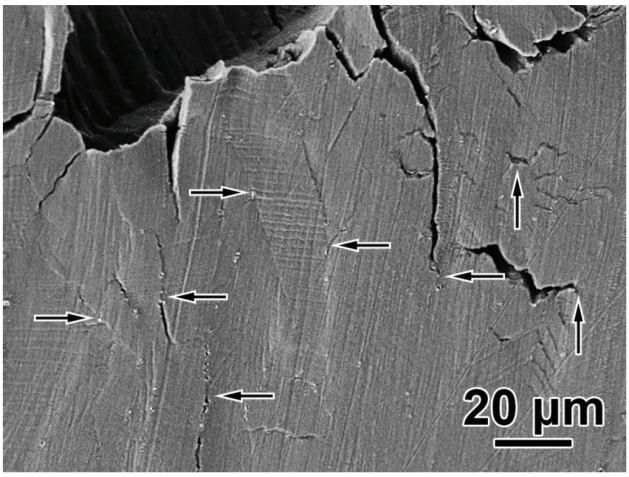


Fig. 11: Laves phases triggering creep crack initiation in AM Inconel 718, illustrating their role in crack tip stress concentration [43].

## V. LIFE PREDICTION MODELS IN CREEP-FATIGUE BEHAVIOR

Particularly in high-temperature settings like power plants, chemical processing equipment and aircraft engines, life prediction models are crucial instruments for evaluating the dependability and durability of components exposed to the combination of creep and fatigue. In addition to cycle-dependent fatigue, these components frequently experience complicated loading conditions that include time-dependent creep, oxidation and microstructural alterations, all of which can have a substantial impact on their operational longevity.

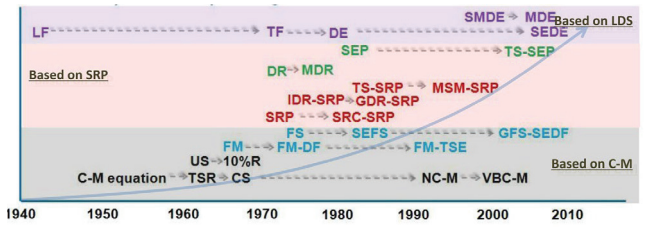


C-M Equation—Coffin-Manson equation (Manson et al,1954)
TSR—Total strain-range model (Halford et al,1964)
FS—Frequency separation model (Coffin et al,1976)
FM—Frequency modified Coffin-Manson (Coffin et al,1969)
FM-DF—Frequency modified damage function (Ostergren,1976)
SRP—Strain-range partitioning method (Coffin et al,1971)
SEP—Strain energy partitioning method (He et al,1979,1983)
IDR-SRP—Interaction Damage Rule SRP (Halford et al, 1976, 1983)
GDR-SRP —Generalized damage rule SRP (Hoffelner, et al 1982)
LF—Life fraction (Miner et al,1945)
TF—Time fraction (Robinson et al,1971)
DE—Ductility exhaustion (Hales et al,1980)
MDE—Modified ductility exhaustion (Splinder et al, 2006)
T-SEDE—Strain energy density exhaustion (Takahashi, 2009)

Fig. 12 - The evolution of traditional creep-fatigue life prediction models throughout time, such as the Coffin-Manson, LDS and SRP methods [46].

### *A. Historical Development and Classification of Life Prediction Models*

Over the last several decades, researchers have introduced over 100 models to predict creep-fatigue life, aiming to account for the complex mechanisms involved in high-temperature service conditions. Fig. 12 presents the progression of foundational creep-fatigue life prediction methods, including the Coffin-Manson relationship, Linear Damage Summation (LDS) and Strain-Range Partitioning (SRP) techniques. This timeline captures the foundational progression from empirical strain-life models to more mechanistic approaches, reflecting the evolving understanding of creep-fatigue interactions. These models can be broadly grouped into three main categories based on their foundational approaches:

*1) Generalization of the Coffin-Manson Equation:* The original Coffin-Manson model established a correlation between plastic strain range ($\Delta\varepsilon_p$) and fatigue life ($N_f$) and was subsequently modified to incorporate inelastic strain range ($\Delta\varepsilon_{in}$) to address creep-fatigue interactions. This extension includes the effects of frequency and dwell time to capture time-dependent damage (Barat et al.). Different strain waveforms, such as those with tensile, compressive, or combined holds, significantly impact the stress-strain response and inelastic strain accumulation, as illustrated by the typical strain-time, stress-time and hysteresis loop plots shown in Fig. 13.

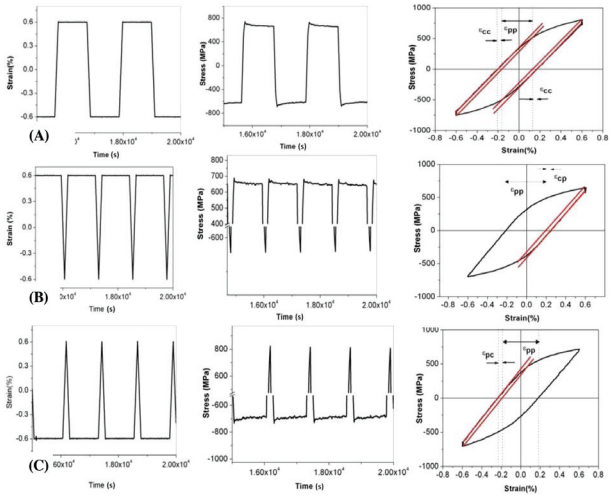


Fig. 13: Typical strain-time, stress-time and hysteresis loops for various hold conditions[12].

Frequency-Modified (FM) Life Model introduces a frequency term (c) to account for dwell times, where the effective strain range is modified by the term $\Delta\varepsilon_{in} \cdot c^{(k-1)}$, accounting for the influence of dwell or hold periods more accurately. The correlation between this frequency-modified factor and the fatigue life in terms of cycles to failure ($N_f$) for GH4169 & Inconel 718, demonstrating how tests under different loading waveforms can be normalized, is shown in Fig. 14 [12], [46].

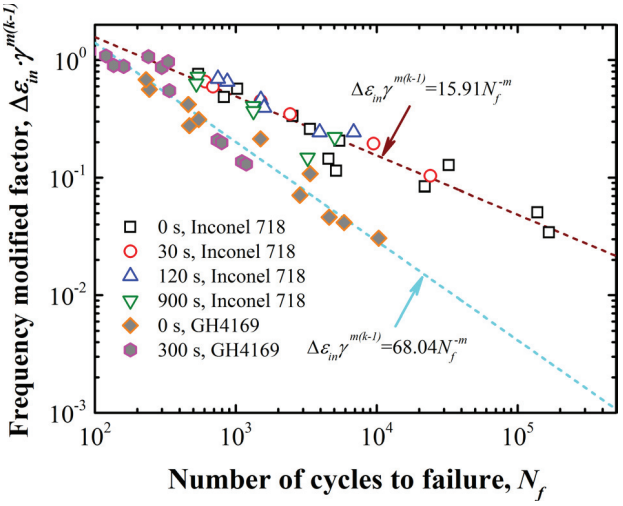


Fig. 14: Correlation of $N_f$ and the FM factor [46].

Frequency-Separation (FS) Life Model further refines this approach by considering separate tension-going and compression-going frequencies, reflecting the different damage potentials during tensile and compressive phases.

Predictions using the FS model for GH4169 & Inconel 718 under HT-LCF, T-CF and C-CF tests are presented in Fig. 15 [12], [46].

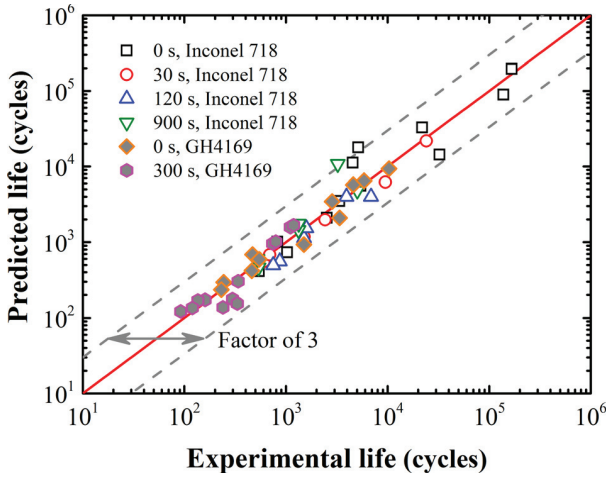


Fig. 15: Creep-fatigue life predictions using the FS model [46]

The Frequency-Modified Damage Function Model (FM-DF Model) builds upon this approach by integrating the maximum tensile stress (σT) into the net tensile hysteretic energy term (σT·Δεin), effectively capturing mean stress effects and enabling more accurate life predictions under various loading waveform conditions. Fig. 16 illustrates the FM-DF model's ability to predict for both Inconel GH4169 & Inconel across various test conditions, including TC-CF tests [12], [46].

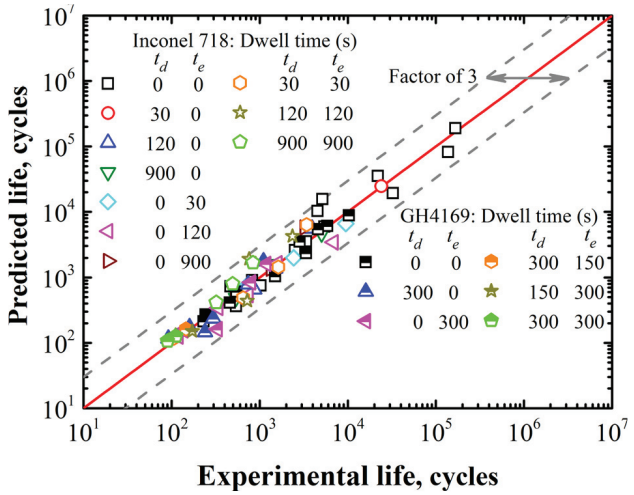


Fig. 16: Creep-fatigue life predictions using the FM-DF model [46].

*2) Generalization of Linear Damage Summation (LDS):*

a) Time Fraction (TF) Model**:** Developed by Miner and Robinson, this model sums the fatigue damage ($N_f/N_{pf}$) and creep damage ($t/t_r$) to estimate total life, assuming damage accumulates independently and linearly. Fig. 17 shows the creep-fatigue predictions and the corresponding damage interaction diagram for GH4169 using the TF model, often compared against the ASME N-47 bilinear envelope [12], [46].

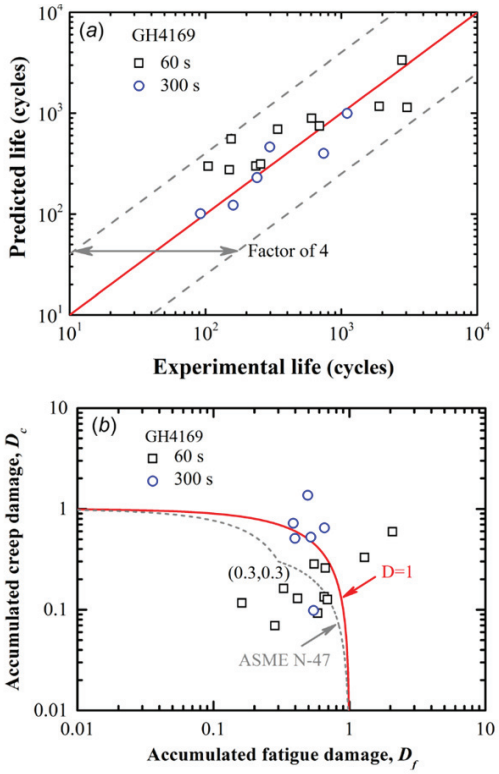


Fig. 17: TF model predictions and damage interaction diagram[46]

b) Ductility Exhaustion (DE) Model**:** Focuses on the exhaustion of creep ductility, where damage is calculated based on the ratio of accumulated creep strain to creep ductility ($\Sigma\epsilon_c/\epsilon_r$), capturing the progressive nature of creep damage. The predictions and damage interaction diagram based on the DE model for GH4169 are shown in Fig. 18 [12], [46].

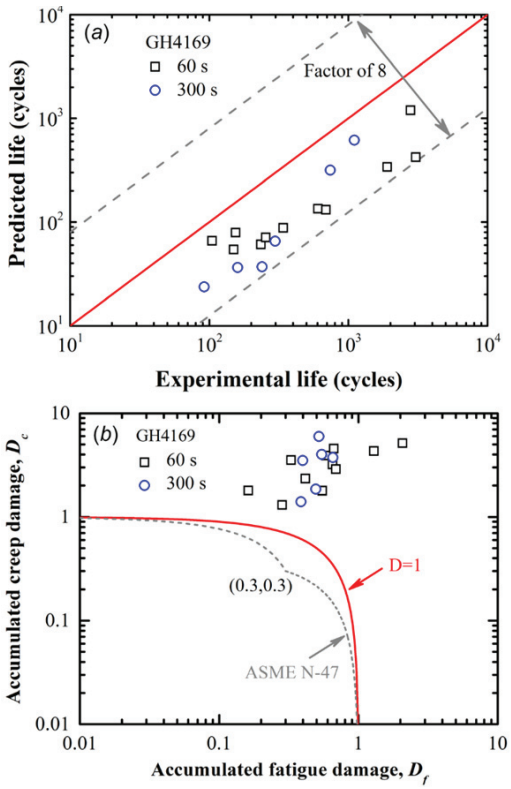


Fig. 18: DE model predictions and damage interaction diagram [46].

*3) Generalization of Strain-Range Partitioning (SRP):*

This approach, first proposed by Manson and Halford, partitions the total inelastic strain range into four components ($\Delta\epsilon_{pp}$, $\Delta\epsilon_{pc}$, $\Delta\epsilon_{cp}$, $\Delta\epsilon_{cc}$) based on whether the strain in tension and compression is plastic or creep, each with distinct damage characteristics. The life relationships for these partitioned strain ranges ($\Delta\epsilon_{ij}$ vs $N_{ij}$) for Inconel 718 and GH4169 are depicted in Fig. 19.

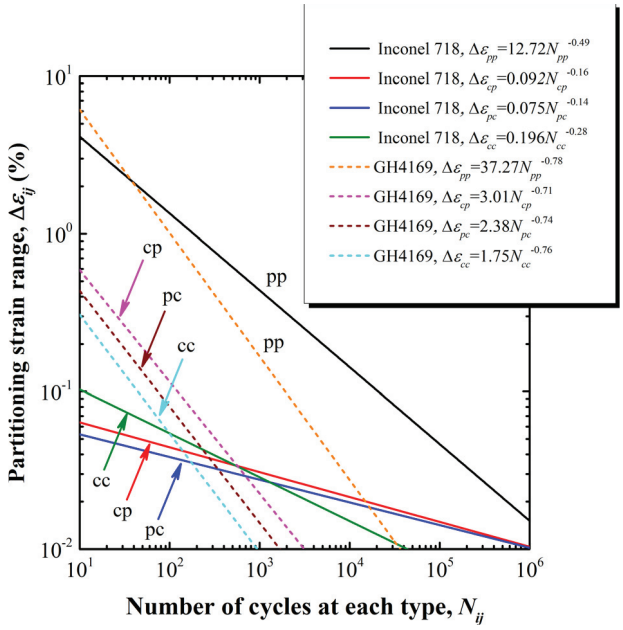


Fig. 19: SRP life relationships for different strain components[46]

It provides a more granular view of creep-fatigue interactions but requires extensive testing to establish material-specific constants. The overall creep-fatigue life predictions using the SRP model for various test conditions are presented in Fig. 20 (Barat et al.).

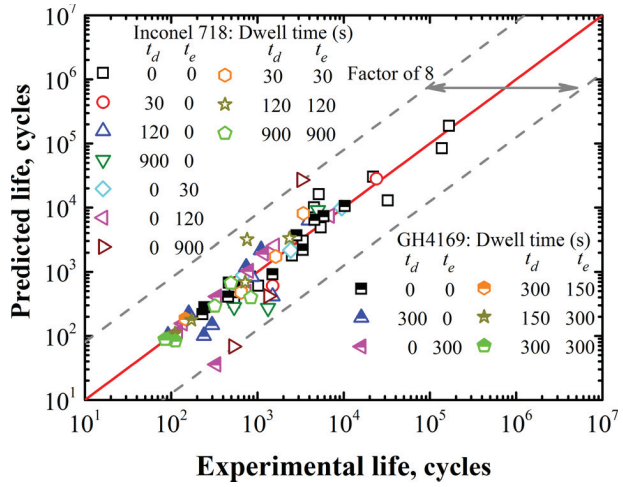


Fig. 20: Creep-fatigue lifetime estimations based on the Strain-Range Partitioning (SRP) model [46]

Strain-Energy Partitioning (SEP) Model**:** An extension of SRP, this method includes the effects of both strain range and maximum stress by considering partitioning strain energy ranges ($\Delta U_{ij}=\sigma_T\cdot\Delta\epsilon_{ij}$), improving life predictions by accounting for the energy dissipated during each cycle. The SEP life relationships ($\Delta U_{ij}$ vs $N_{ij}$) are shown in Fig. 21 (a) along with the associated life predictions are in Fig. 21 (b) of that paper, generally showing better correlation than SRP.

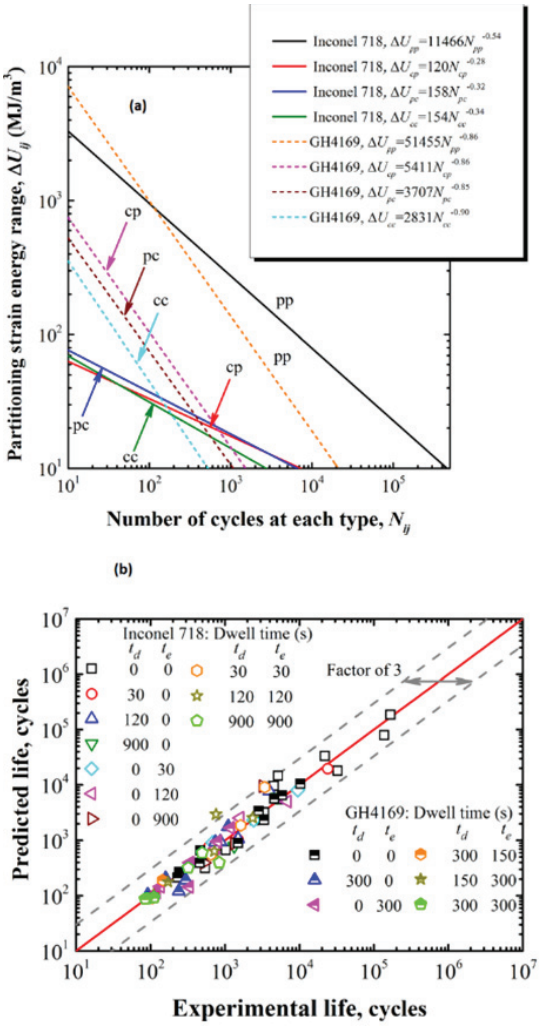


Fig. 21: (a) SEP life relationships (b), Creep-fatigue life predictions using the SEP model [46].

*B. Walker-Based Model for Predicting Creep-Fatigue Life*

In addition to these conventional models, recent advancements have focused on improving prediction accuracy through better incorporation of dwell and stress ratio effects. One such approach is the Walker Total Strain Equation, which extends the classic Morrow equation by introducing strain ratio correction (Wang et al.):

$$\Delta\epsilon = \left(\frac{\sigma_f'}{E}\right)(2N_f)^b + \epsilon_f'(2N_f)^c$$

where:

$\Delta\epsilon$ = total strain range

$\sigma_f'$ = coeff. of fatigue strength

$\epsilon_f'$ = coeff. of fatigue ductility

$E$ = elastic modulus

$b$ = fatigue strength exponent

$c$ = fatigue ductility exponent

Recent adaptations, such as Walker's model, incorporated strain ratio corrections to account for the influence of varying stress ratios. (Wang et al.):

$$\Delta\epsilon = \left(\frac{\sigma_f'}{E}\right)(2N_f)^{b_{new}} + \epsilon_f'(2N_f)^{c_{new}}$$

where the coefficients $b_{new}$ and $c_{new}$ are adjusted based on dwell time, capturing the increased damage accumulation during dwell periods. The effect of revising these exponents based on dwell time on the total strain equation for FGH96 is illustrated in Fig. 22.

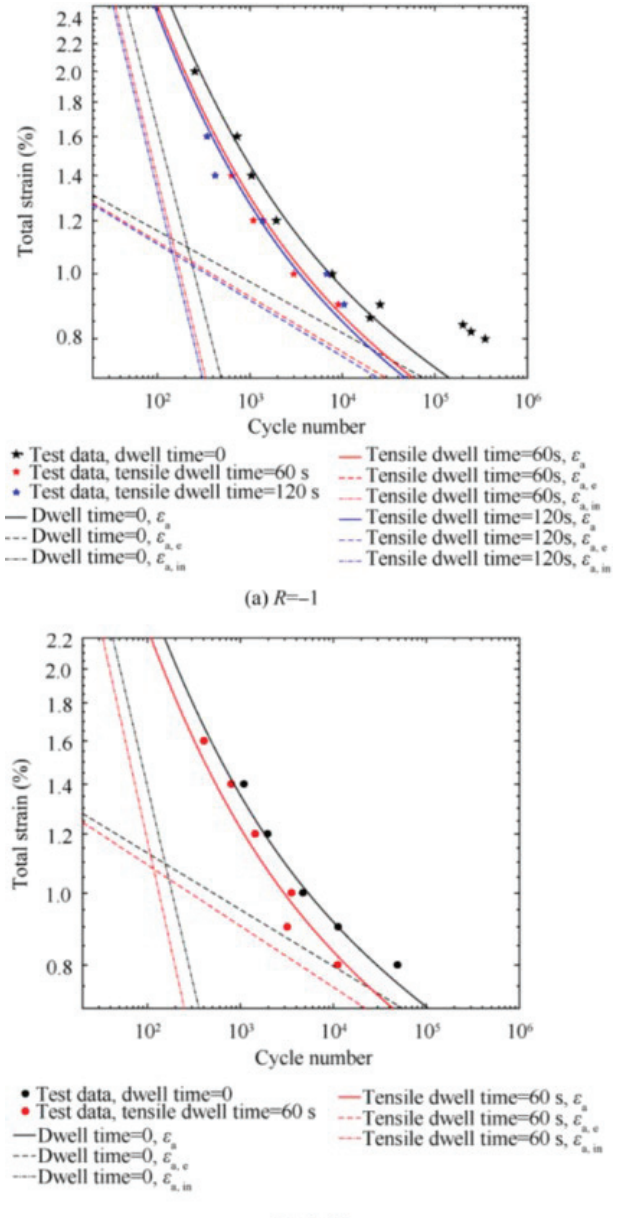


Fig. 22: Effect of $b_{new}$ and $c_{new}$ revision on the Walker total strain equation [34].

This modification enables the model to address fatigue behaviour (both HCF & HCF), increasing its versatility across diverse engineering applications without the need for extensive supplemental creep testing (Wang et al.). Fig. 23 presents a comparison between experimental results and predicted fatigue life using the updated CFI model for FGH96, GH4169 and FGH95.

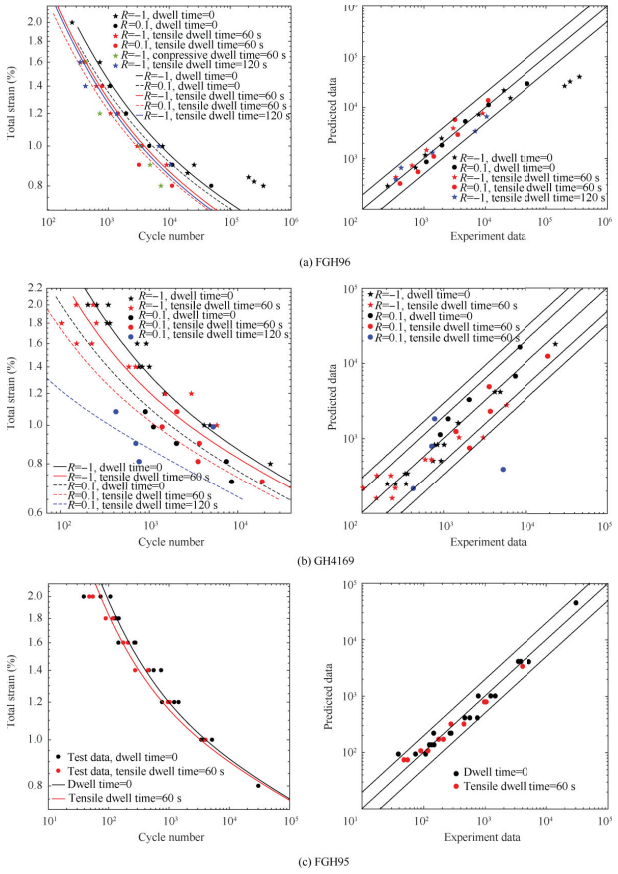


Fig. 23: Comparison between experimental results and predicted fatigue life using the Walker-based CFI model [34]

## C. *Energy-Based Models*

*1) Inelastic Strain Energy-Based Model (Chen et al.):* This model connects fatigue life to the amount of energy dissipated in each cycle, based on the assumption that a fraction of this energy leads to irreversible material damage. (Barat et al.):

$$N_f = \frac{C}{\left(\frac{\sigma_{\max}\Delta\epsilon_{\text{in}}}{\Delta W}\right)^m \Delta W_0}$$

The variable $N_f$ refers to the total number of cycles until failure, $\Delta\epsilon_{\text{in}}$ indicates the inelastic strain amplitude, $\sigma_{\max}$ is the highest tensile stress experienced and $\Delta W$ represents the energy dissipated through hysteresis in each cycle. The parameters $C$ and $m$ are constants specific to the material (Chen et al.). Fig. 24 compares the model's predicted fatigue life with experimental results for Inconel 718 under various complex loading waveforms.

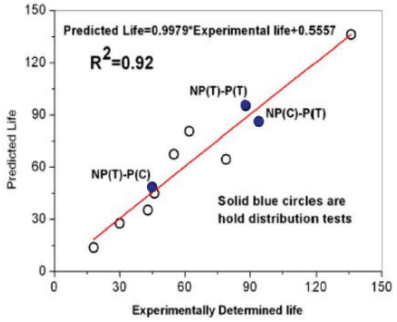


Fig. 24: Life prediction using the modified Chen et al. energy-based model [12]

*2) Hysteresis Energy Failure Density Approach (Oldham and Abou-Hanna):* This method uses the concept of intrinsic hysteresis energy to predict fatigue life (Barat et al.):

$$N_f = \frac{E_{\text{intrinsic}}}{W}$$

where $E_{\text{intrinsic}}$ represents the average cumulative hysteresis energy density accumulated over the entire fatigue life, while $W$ denotes the energy dissipated during a single loading cycle. The method often involves deconvoluting creep and plastic energy contributions, as schematically shown for determining these energy fractions from an inelastic loop in Fig. 25 (Barat et al.).

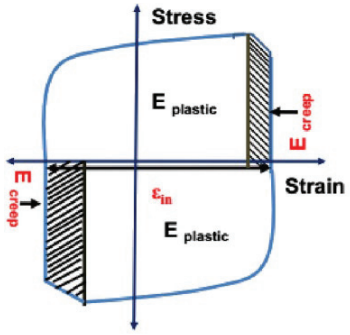


Fig. 25: Scheme for determining plastic and creep energy fractions [12].

*3) Viscosity-Based Models (Zhu et al.):* These models account for time-dependent viscous effects [47]:

$$N_f = C\left(\Delta W_p\, \sigma_{\max}^{1+n'}\right)^{-\frac{1}{\beta(1+n')}} \left(E_p - t\,\Delta W_{\text{FL}}\right)^{\frac{\alpha}{\beta(1+n')}}$$

Where the parameters are defined as:

$\Delta W_p$: Inelastic energy density per cycle (plastic + creep)

$\sigma_{\max}$ : Maximum tensile stress in the cycle

$n'$: Strain hardening exponent (viscosity-related parameter)

β: Damage accumulation exponent

α: Material-specific scaling factor

t: Time duration (cycle-dependent)

C: Material constant (empirically determined)

The term $E_p$ is a viscosity-based parameter defined as:

$$E_p = t_d\sigma_{\max} + (t_d + t_c + t_h)\sigma_{\min}H(\sigma_{\min}) + \frac{t_c + t_h}{2} f(\sigma_{\max}, \sigma_{\min})$$

Where:

$t_d$: Duration of dynamic loading

$t_c$: Duration of compressive dwell

$t_h$: Duration of tensile dwell

$\sigma_{\min}$: Minimum stress in the cycle

$H(\sigma_{\min})$: Step function that activates based on whether $\sigma_{\min}$ contributes to damage

$f(\sigma_{\max}, \sigma_{\min})$: Stress conversion function used for cyclic asymmetry correction

And:

$$\Delta W_{\text{FL}} = \frac{\sigma_{\text{lim}}^2}{2E}$$

Where:

$\sigma_{\text{lim}}$: Fatigue limit stress (below which no damage is assumed)

*D. Young's modulus (elastic modulus of the material)*

Life prediction models play a vital role in ensuring the reliability and cost-efficiency of components operating under elevated temperature environments. Continued refinement of these models aims to improve their accuracy, reduce conservatism and better reflect real-world conditions, ensuring their ongoing relevance in critical engineering applications. For instance, understanding how different waveforms (e.g., those with peak holds, non-peak holds, or variable strain rates) affect the material's response is key. Fig. 26 presents a representative fatigue-creep loading scenario featuring a tensile dwell, a condition these models are specifically designed to evaluate.

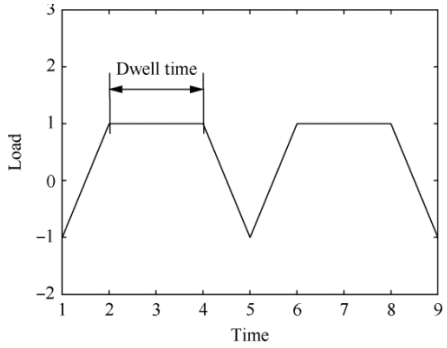


Fig. 26: Representative fatigue-creep loading profile featuring a tensile dwell period. [34].

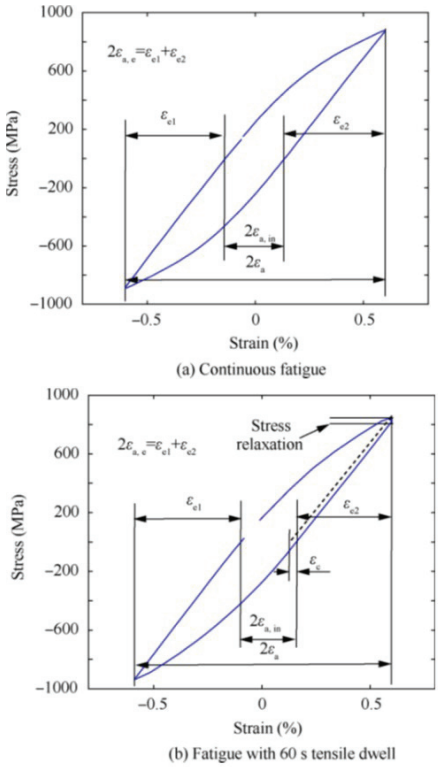


Fig. 27: Schematic of strain components in hysteresis loops [34].

The resulting inelastic hysteresis loops, such as those shown schematically in Fig. 27 provide data on strain components which are fundamental inputs for many models.

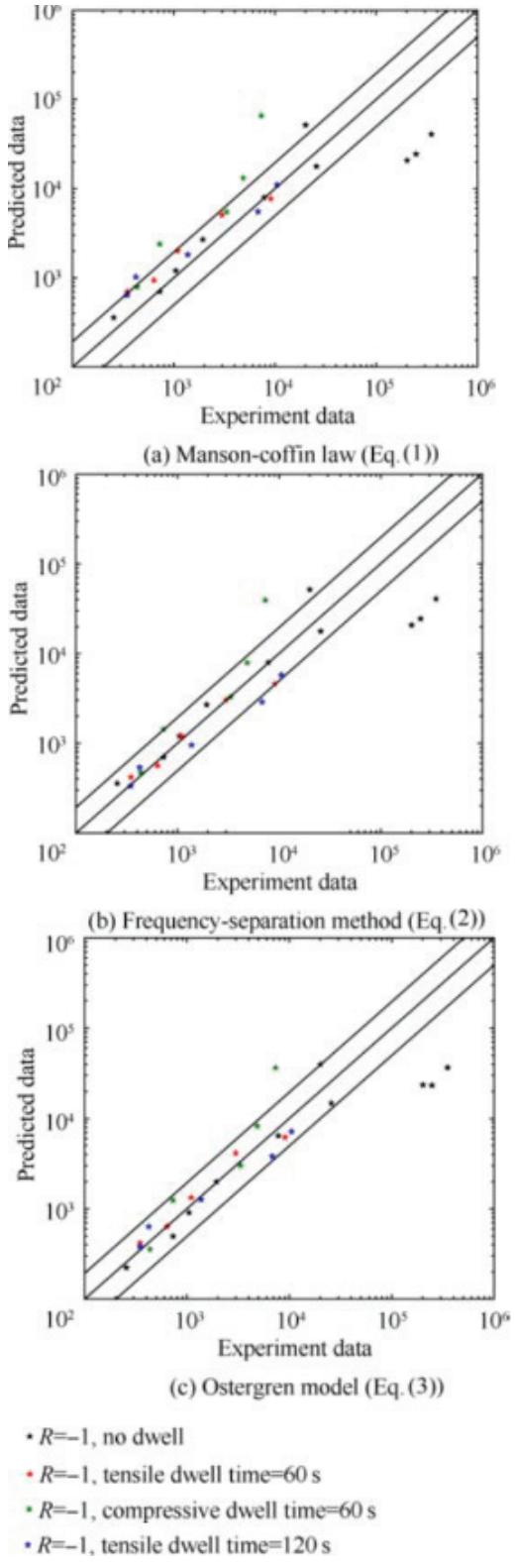


Fig. 28: Comparison of traditional model predictions for FGH96[34].

The success of any model is often validated by comparing its predictions against experimental data, as seen in Fig. 28, where the cyclic life predictions for FGH96 by three traditional models are compared with test data, highlighting the varying degrees of accuracy and the limitations that necessitate the development of more advanced models like the Walker-based approaches discussed. This iterative process of model development, validation against experimental results and refinement is essential for advancing the field of creep-fatigue life prediction.

Most existing creep-fatigue life prediction models for Inconel 718 demonstrate accuracy within the commonly accepted ±2X scatter band, but their reliability decreases when applied to AM alloys with anisotropy, residual stresses, and process-induced defects. While energy-based and mechanism-based models often yield better correlations under dwell conditions, empirical strain-life models remain limited by their dependence on extensive testing. Overall, quantitative validation remains scarce for AM-specific conditions, indicating the need for systematic benchmarking studies.

Although conventional life prediction models provide reasonable accuracy for wrought Inconel 718, their transferability to AM counterparts is limited. Recent work on EBM-processed Inconel 718 has shown that fatigue life predictions based on traditional strain-based formulations exhibit greater scatter, reflecting the influence of anisotropy, porosity, and residual stresses. Moreover, dwell-induced intergranular cracking, commonly observed in AM materials, is not adequately represented in conventional models. These observations highlight the need for developing AM-specific life prediction frameworks that explicitly incorporate microstructural features and defect populations.

## VI. CRITICAL KNOWLEDGE GAPS AND CHALLENGES

Although significant research has been conducted on creep-fatigue behavior in conventionally processed Inconel 718, its applicability to additively manufactured (AM) components remains limited due to fundamental differences in microstructure, defect types and residual stress profiles. Several key knowledge gaps and practical challenges still need to be addressed:

### *A. Lack of Comprehensive Studies on AM-Specific Creep-Fatigue Behavior*

Creep-fatigue interaction has long been studied in conventionally forged or cast Inconel 718, but its behavior in AM variants remains underexplored. The distinct microstructural features of additively manufactured (AM) materials—such as columnar grain structures aligned with the build direction, the presence of residual Laves and δ phases and varying levels of porosity—have a significant impact on time-dependent deformation and crack propagation. However, these effects are not yet comprehensively addressed in existing literature.

### *B. Evolving Standards for Mechanical Testing*

Mechanical testing standards specifically designed for additively manufactured (AM) materials are still under development, especially when it comes to evaluating performance in high-temperature environments. There is a lack of universally accepted testing protocols that account for AM-induced anisotropy, residual stresses and defect distributions during creep-fatigue interaction studies. Conventional standards may not accurately reflect the service conditions or failure modes encountered in AM components.

### *C. Microstructural Anisotropy and Its Impact on Damage Evolution*

Additive manufacturing results in anisotropic properties, stemming from the layer-by-layer fabrication approach, which causes the material behavior to vary based on build orientation. This anisotropy significantly influences crack initiation and growth during creep-fatigue loading, yet there is limited experimental data correlating build orientation with fatigue and creep performance in AM Inconel 718.

### *D. Influence of Defects and Limited Data on Their Criticality*

While porosity, lack-of-fusion defects and unmelted particles are frequently observed in additive manufacturing processes, there is a limited amount of quantitative data linking these defects to the creep-fatigue life of the material. The critical size or distribution of these defects that trigger failure is not clearly defined, making defect tolerance criteria difficult to establish.

### *E. Inadequate Post-Processing Guidelines for Creep-Fatigue Optimization*

While techniques like heat treatment and Hot Isostatic Pressing (HIP) are effective in enhancing the creep and fatigue behavior of materials, there is currently no standardized approach specifically designed to optimize creep-fatigue resistance in additively manufactured Inconel 718.Inconsistencies in thermal treatments can result in over-aging, excessive grain boundary precipitation, or incomplete phase dissolution, each affecting long-term performance.

## VII. FUTURE RESEARCH DIRECTIONS

To support the safe and reliable deployment of additively manufactured (AM) Inconel 718 in elevated temperature environment applications, future research should focus on establishing AM-specific understanding, improving process control and enabling predictive performance modeling. The following directions outline key priorities:

### *A. Establishing AM-Specific Creep-Fatigue Baselines*

While creep-fatigue interaction has been widely studied in conventionally processed materials, its behavior in AM Inconel 718 is still emerging. There is a need to generate comprehensive baseline data under representative conditions, including low-cycle fatigue (LCF) tests with dwell times that reflect real service environments. These studies should consider variations in build orientation, loading waveform and post-processing states.

### *B. Advancing Standardized Testing Frameworks*

Mechanical testing protocols must evolve to account for the unique microstructures and defect profiles of AM materials. There is significant opportunity to contribute to the development of standardized testing procedures (e.g., ASTM, ISO) that incorporate strain rate effects, dwell hold types and anisotropy considerations. Defining test strategies specific to AM variants will improve cross-study comparisons and accelerate material qualification.

### *C. Microstructural Mechanism Mapping*

Detailed investigation into how microstructural features—such as grain orientation, phase distribution and residual segregation—impact damage evolution is essential. Focused studies using microscopy, phase analysis and mechanical property correlation can clarify how different AM process parameters influence long-term performance, particularly under creep-fatigue loading.

### *D. Developing Practical Life Prediction Models*

To support design and reliability assessment, future work should aim to develop physics-informed, scalable life prediction models. These models should incorporate inputs such as inelastic strain energy, stress relaxation characteristics and cyclic softening behavior—parameters that are accessible through standard testing and characterization methods. This will facilitate more accurate and accessible service life estimation for AM components.

### *E. Optimization of Post-Processing for Creep-Fatigue Performance*

Heat treatments and HIP cycles processes are essential for refining the microstructure of AM Inconel 718. Future research should aim to systematically optimize post-processing protocols to balance residual stress relief, phase precipitation ($\gamma'$, $\gamma''$) and defect healing without compromising mechanical integrity. Understanding the impact of different thermal histories on creep-fatigue resistance will be key to adapting treatments for specific application requirements.

### *F. Impact of Oxidation on Creep-Fatigue Behavior*

Oxidation is a key environmental factor influencing creep-fatigue interactions at elevated temperatures. Oxidation-assisted grain boundary embrittlement accelerates intergranular crack initiation, particularly during tensile dwell periods. In AM Inconel 718, columnar grains aligned with the build direction and δ-phase precipitation along grain boundaries may further exacerbate this susceptibility. While such effects have been well documented in conventionally processed superalloys, systematic studies on AM microstructures remain limited. Future work should focus on quantifying the role of oxidation in dwell-sensitive crack growth to develop more reliable life prediction models for AM components.

*Critical Research Gaps:*

- Limited experimental datasets for creep-fatigue in AM Inconel 718, especially under multiaxial and thermomechanical loading.
- Inadequate understanding of the interaction between oxidation, dwell time, and AM-specific microstructures.
- Lack of AM-specific life prediction models that capture anisotropy, porosity, and residual stresses.
- Scaling challenges in post-processing treatments (heat treatment, HIP) for industrial adoption.
- Limited integration of advanced computational tools (digital twins, physics-informed ML) into life prediction frameworks.

Machine learning and data-driven approaches are increasingly being applied to fatigue and creep-fatigue life prediction. Early studies demonstrate the potential of symbolic regression, surrogate models, and digital twins to predict life with higher accuracy compared to conventional empirical models. For AM Inconel 718, such approaches could enable better use of small experimental datasets by leveraging microstructural descriptors and process history as inputs. However, their success depends on the availability of standardized datasets and careful validation against experimental scatter bands.

## VIII. CONCLUSION

In the aerospace and energy industries, where fatigue resistance and high-temperature creep are critical, Inconel 718 components are being fabricated using additive manufacturing (AM) more and more. Conventionally made Inconel 718 has a well-studied creep-fatigue behavior, but AM variations provide special difficulties because of their different microstructures, which include columnar grains, Laves and δ phases, anisotropy and intrinsic flaws such porosity and lack-of-fusion. These features significantly influence time-dependent deformation and damage evolution, necessitating a focused investigation of their impact under combined cyclic and creep loading.

This review provides a comprehensive assessment of the creep-fatigue interaction in AM Inconel 718. It explores how AM-induced features affect crack initiation and growth, outlines current testing approaches and evaluates life prediction models. While models such as Coffin-Manson, Linear Damage Summation and energy-based methods offer foundational insights, they often fail to account for AM-specific behaviors such as anisotropic softening, stress relaxation and microstructural evolution.

Key knowledge gaps include the lack of AM-specific creep-fatigue datasets, evolving testing standards, insufficient understanding of microstructural anisotropy and limited guidelines for post-processing. Future studies should concentrate on creating baseline performance data, improving testing procedures, creating scalable predictive models and refining thermal treatments to improve performance consistency in order to overcome these issues. By bringing together the current understanding of mechanisms, modeling and challenges, this review lays the groundwork for advancing the reliability and design of AM Inconel 718 components in demanding service conditions.

## DATA AVAILABILITY

The data generated or analyzed during the current study can be accessed from the corresponding author upon justified request.

## COMPETING INTERESTS

The authors affirm that there are no financial or personal conflicts that could have influenced the outcomes or interpretations presented in this research.

## ACKNOWLEDGMENTS

The authors gratefully acknowledge the support and infrastructure provided by Savitribai Phule Pune University, Pune, as well as Amrutvahini College of Engineering, Sangamner, District Ahilyanagar (M.S.), IN, which were instrumental in carrying out this work.

## REFERENCES

[1] S. Guth, T. Babinsk\`y, S. Antusch, A. Klein, D. Kuntz, and I. Šulák, “Creep–Fatigue interaction of Inconel 718 manufactured by electron beam melting,” *Adv Eng Mater*, vol. 25, no. 16, p. 2300294, 2023.

[2] E. Akca and A. Gürsel, “A Review on Superalloys and IN718 Nickel-Based INCONEL Superalloy,” *Periodicals of Engineering and Natural Sciences (PEN)*, vol. 3, no. 1, Jun. 2015, doi: 10.21533/pen.v3i1.43.

[3] J. Y. Guédou, I. Augustins-Lecallier, L. Nazé, P. Caron, and D. Locq, “Development of a new fatigue and creep resistant PM nickel-base superalloy for disk applications,” in *Proceedings of the International Symposium on Superalloys*, Minerals, Metals and Materials Society, 2008, pp. 21–30. doi: 10.7449/2008/superalloys_2008_21_30.

[4] S. B. and W. V. D. Chaudhari, “A Comprehensive Review on the High-Temperature Behavior of Additively Manufactured Inconel 718,” in *Recent Advances in Additive Manufacturing, Volume 1*, S. and C. B. S. Mallaiah Manjaiah and Thapliyal, Ed., Singapore: Springer Nature Singapore, 2025, pp. 439–524. doi: 10.1007/978-981-97-6016-9_34.

[5] J. J. Shi *et al.*, “Microstructure and creep anisotropy of Inconel 718 alloy processed by selective laser melting,” *Materials Science and Engineering: A*, vol. 805, p. 140583, 2021, doi: https://doi.org/10.1016/j.msea.2020.140583.

[6] Z. Wang, W. Wu, J. Liang, and X. Li, “Creep–fatigue interaction behavior of nickel-based single crystal superalloy at high temperature by in-situ SEM observation,” *Int J Fatigue*, vol. 141, p. 105879, 2020.

[7] J. K. S. Jadon, R. Singh, and J. K. Mahato, “Creep-fatigue interaction behavior of high temperature alloys: A review,” *Mater Today Proc*, vol. 62, pp. 5351–5357, 2022.

[8] K. N. Amato *et al.*, “Microstructures and mechanical behavior of Inconel 718 fabricated by selective laser melting,” *Acta Mater*, vol. 60, no. 5, pp. 2229–2239, Mar. 2012, doi: 10.1016/j.actamat.2011.12.032.

[9] Y.-L. Kuo, T. Nagahari, and K. Kakehi, “The Effect of Post-Processes on the Microstructure and Creep Properties of Alloy718 Built Up by Selective Laser Melting,” *Materials*, vol. 11, no. 6, 2018, doi: 10.3390/ma11060996.

[10] G. Bryndza *et al.*, “Review of the Microstructural Impact on Creep Mechanisms and Performance for Laser Powder Bed Fusion Inconel 718,” *Materials*, vol. 18, no. 2, 2025, doi: 10.3390/ma18020276.

[11] A. R. Balachandramurthi *et al.*, “On the Microstructure of Laser Beam Powder Bed Fusion Alloy 718 and Its Influence on the Low Cycle Fatigue Behaviour,” *Materials*, vol. 13, no. 22, 2020, doi: 10.3390/ma13225198.

[12] K. Barat, S. Sivaprasad, S. K. Kar, and S. Tarafder, “Low-cycle fatigue of IN 718: Effect of waveform,” *Fatigue Fract Eng Mater Struct*, vol. 42, no. 12, pp. 2823–2843, 2019.

[13] P. D. Nezhadfar, A. S. Johnson, and N. Shamsaei, “Fatigue behavior and microstructural evolution of additively manufactured Inconel 718 under cyclic loading at elevated temperature,” *Int J Fatigue*, vol. 136, p. 105598, 2020, doi: https://doi.org/10.1016/j.ijfatigue.2020.105598.

[14] J. J. Shi *et al.*, “Study on the microstructure and creep behavior of Inconel 718 superalloy fabricated by selective laser melting,” *Materials Science and Engineering: A*, vol. 765, p. 138282, 2019, doi: https://doi.org/10.1016/j.msea.2019.138282.

[15] C. J. Gibson, “Creep Fatigue Crack Growth Behavior of Wrought and Additive Manufactured IN718 at Elevated Temperature,” University of Idaho, 2021.

[16] T. Nagahari, T. Nagoya, K. Kakehi, N. Sato, and S. Nakano, “Microstructure and Creep Properties of Ni-Base Superalloy IN718 Built up by Selective Laser Melting in a Vacuum Environment,” *Metals (Basel)*, vol. 10, no. 3, 2020, doi: 10.3390/met10030362.

[17] N. Sonntag *et al.*, “Tensile and Low-Cycle Fatigue Behavior of Laser Powder Bed Fused Inconel 718 at Room and High Temperature,” *Adv Eng Mater*, vol. 26, no. 10, p. 2302122, 2024, doi: https://doi.org/10.1002/adem.202302122.

[18] S. Sui, J. Chen, E. Fan, H. Yang, X. Lin, and W. Huang, “The influence of Laves phases on the high-cycle fatigue behavior of laser additive manufactured Inconel 718,” *Materials Science and Engineering: A*, vol. 695, pp. 6–13, 2017, doi: https://doi.org/10.1016/j.msea.2017.03.098.

[19] Z. Xu, J. W. Murray, C. J. Hyde, and A. T. Clare, “Effect of post processing on the creep performance of laser powder bed fused Inconel 718,” *Addit Manuf*, vol. 24, pp. 486–497, 2018, doi: https://doi.org/10.1016/j.addma.2018.10.027.

[20] J. J. Shi *et al.*, “Microstructure and creep anisotropy of Inconel 718 alloy processed by selective laser melting,” *Materials Science and Engineering: A*, vol. 805, p. 140583, 2021, doi: https://doi.org/10.1016/j.msea.2020.140583.

[21] R. Barros *et al.*, “Laser Powder Bed Fusion of Inconel 718: Residual Stress Analysis Before and After Heat Treatment,” *Metals (Basel)*, vol. 9, no. 12, 2019, doi: 10.3390/met9121290.

[22] Z. Luo, Z. Wang, Z. Yan, J. Chen, S. Li, and M. Liu, “Formation of defects in selective laser melted Inconel 718 and its correlation with mechanical properties through dimensionless numbers,” *Sci China Phys Mech Astron*, vol. 65, no. 5, p. 254611, 2022, doi: 10.1007/s11433-021-1861-1.

[23] A. M. Kiss *et al.*, "Laser-induced keyhole defect dynamics during metal additive manufacturing," *Adv Eng Mater*, vol. 21, no. 10, p. 1900455, 2019.

[24] J. P. Pi~dron and A. Pineau, "The Effect of Microstructure and Environment on the Crack Growth Behaviour of Inconel 718 Alloy at 650 °C under Fatigue, Creep and Combined Loading," 1982.

[25] W. Schneller, M. Leitner, S. Springer, F. Grün, and M. Taschauer, "Effect of hip treatment on microstructure and fatigue strength of selectively laser melted AlSi10Mg," *Journal of Manufacturing and Materials Processing*, vol. 3, no. 1, Mar. 2019, doi: 10.3390/jmmp3010016.

[26] L. Li, X. Zhu, F. Tian, Y. Chen, and Q. Liu, "Effect of annealing treatment on mechanical and fatigue properties of Inconel 718 alloy melted by selective laser melting," *Matéria (Rio de Janeiro)*, vol. 27, 2022.

[27] K. Feng, P. Liu, H. Li, S. Sun, S. Xu, and J. Li, "Microstructure and phase transformation on the surface of Inconel 718 alloys fabricated by SLM under 1050°C solid solution + double ageing," *Vacuum*, vol. 145, pp. 112–115, 2017, doi: https://doi.org/10.1016/j.vacuum.2017.08.044.

[28] D. B. Witkin, D. N. Patel, H. Helvajian, L. Steffeney, and A. Diaz, "Surface Treatment of Powder-Bed Fusion Additive Manufactured Metals for Improved Fatigue Life," *J Mater Eng Perform*, vol. 28, no. 2, pp. 681–692, Feb. 2019, doi: 10.1007/s11665-018-3732-9.

[29] H.-H. Gu, X.-C. Zhang, K. Zhang, K.-S. Li, S.-T. Tu, and R.-Z. Wang, "A novel fatigue and creep-fatigue life prediction model by combining data-driven approach with domain knowledge," *Int J Fatigue*, vol. 186, p. 108402, 2024, doi: https://doi.org/10.1016/j.ijfatigue.2024.108402.

[30] S. Mukherjee, S. K. Kar, S. Sivaprasad, S. Tarafder, G. B. Viswanathan, and H. L. Fraser, "Creep-fatigue response, failure mode and deformation mechanism of HAYNES 282 Ni based superalloy: effect of dwell position and time," *Int J Fatigue*, vol. 159, p. 106820, 2022.

[31] R. Z. Wang, X. C. Zhang, J. G. Gong, X. M. Zhu, S. T. Tu, and C. C. Zhang, "Creep-fatigue life prediction and interaction diagram in nickel-based GH4169 superalloy at 650 °C based on cycle-by-cycle concept," *Int J Fatigue*, vol. 97, pp. 114–123, Apr. 2017, doi: 10.1016/j.ijfatigue.2016.11.021.

[32] G. Chen, Y. Zhang, D. K. Xu, Y. C. Lin, and X. Chen, "Low cycle fatigue and creep-fatigue interaction behavior of nickel-base superalloy GH4169 at elevated temperature of 650 C," *Materials Science and Engineering: A*, vol. 655, pp. 175–182, 2016.

[33] A. Shanyavskiy, V. Shlyannikov, A. Soldatenkov, and V. Rubtsov, "Micromechanics of fatigue, creep-fatigue interaction and thermo-mechanical crack growth of XH73M nickel alloy," *Procedia Structural Integrity*, vol. 43, pp. 215–220, 2023.

[34] C. Siyuan, W. E. I. Dasheng, W. Jialiang, W. Yanrong, and others, "A new fatigue life prediction model considering the creep-fatigue interaction effect based on the Walker total strain equation," *Chinese Journal of Aeronautics*, vol. 33, no. 9, pp. 2382–2394, 2020.

[35] D. Sun, G. Ma, Z. Wan, and J. Gao, "Study on creep-fatigue interaction mechanism and life prediction of aero-engine turbine blade," *Eng Fail Anal*, vol. 154, p. 107715, 2023.

[36] S. Kim, H. Choi, J. Lee, and S. Kim, "Room and elevated temperature fatigue crack propagation behavior of Inconel 718 alloy fabricated by laser powder bed fusion," *Int J Fatigue*, vol. 140, p. 105802, 2020, doi: https://doi.org/10.1016/j.ijfatigue.2020.105802.

[37] H. Ostergaard, J. Pribe, M. T. Hasib, T. Siegmund, and J. Kruzic, "Crack growth in laser powder bed fusion fabricated alloy 718 at 650 °C under static and cyclic loading," *Int J Fatigue*, vol. 193, p. 108810, May 2025, doi: 10.1016/j.ijfatigue.2025.108810.

[38] R. Konečná, L. Kunz, G. Nicoletto, and A. Bača, "Fatigue crack growth behavior of Inconel 718 produced by selective laser melting," *Int J Fatigue*, vol. 10, pp. 31–40, May 2016, doi: 10.3221/IGF-ESIS.36.04.

[39] E. Sadeghi, P. Karimi, N. Israelsson, J. Shipley, T. Månsson, and T. Hansson, "Inclusion-induced fatigue crack initiation in powder bed fusion of Alloy 718," *Addit Manuf*, vol. 36, p. 101670, 2020, doi: https://doi.org/10.1016/j.addma.2020.101670.

[40] E. Sadeghi, G. Asala, P. Karimi, D. Deng, J. Moverare, and T. Hansson, "Fatigue crack initiation and propagation in Alloy 718 with a bimodal grain morphology built via electron beam-powder bed fusion," *Materials Science and Engineering: A*, vol. 827, p. 142051, 2021, doi: https://doi.org/10.1016/j.msea.2021.142051.

[41] M. Prost *et al.*, "Anisotropy in cyclic behavior and fatigue crack growth of IN718 processed by laser powder bed fusion," *Addit Manuf*, vol. 61, p. 103301, 2023, doi: https://doi.org/10.1016/j.addma.2022.103301.

[42] K. Gruber *et al.*, "Fatigue crack growth characterization of Inconel 718 after additive manufacturing by laser powder bed fusion and heat treatment," *Int J Fatigue*, vol. 166, p. 107287, 2023, doi: https://doi.org/10.1016/j.ijfatigue.2022.107287.

[43] T. Ma, G.-P. Zhang, P. Tan, and B. Zhang, "Effects of homogenization temperature on creep performance of laser powder bed fusion-fabricated Inconel 718 at 650 °C," *Materials Science and Engineering: A*, vol. 853, p. 143794, 2022, doi: https://doi.org/10.1016/j.msea.2022.143794.

[44] S. Zhang *et al.*, "The creep behavior of IN718 alloy fabricated by selective laser melting compared to forging," *Appl Mater Today*, vol. 38, p. 102252, 2024, doi: https://doi.org/10.1016/j.apmt.2024.102252.

[45] B. Vieille *et al.*, "Investigations on the fracture behavior of Inconel 718 superalloys obtained from cast and additive manufacturing processes," *Materials Science and Engineering: A*, vol. 790, p. 139666, 2020, doi: https://doi.org/10.1016/j.msea.2020.139666.

[46] R. Z. Wang, J. Wang, J. G. Gong, X. C. Zhang, S. T. Tu, and C. C. Zhang, "Creep-Fatigue Behaviors and Life Assessments in Two Nickel-Based Superalloys," *Journal of Pressure Vessel Technology, Transactions of the ASME*, vol. 140, no. 3, Jun. 2018, doi: 10.1115/1.4039779.

[47] S.-P. Zhu, H.-Z. Huang, H. Li, R. Sun, and M. J. Zuo, "A New Ductility Exhaustion Model for High Temperature Low Cycle Fatigue Life Prediction of Turbine Disk Alloys," vol. 28, no. 2, pp. 119–131, 2011, doi: doi:10.1515/tjj.2011.011.